Acta Med. Okayama, 2022
Vol. 76, No. 5, pp. 511–517

Acta Medica Okayama
http://escholarship.lib.okayama-u.ac.jp/amo/

Original Article

Effects of Model-Based Iterative Reconstruction in Low-Dose Paranasal Computed Tomography: A Comparison with Filtered Back Projection and Hybrid Iterative Reconstruction

Hayato Tomita[a]*, Kenji Kuramochi[a], Atsuko Fujikawa[a], Hirotaka Ikeda[b], Midori Komita[a], Yoshiko Kurihara[c], Yasuyuki Kobayashi[d], and Hidefumi Mimura[a]

Departments of [a]Radiology, [d]Advanced Biomedical Imaging Informatics, St. Marianna University School of Medicine, Kawasaki, Kanagawa 216-8511, Japan, [b]Department of Radiology, Fujita Health University School of Medicine, Toyoake, Aichi 470-1192, Japan, [c]Department of Radiology, Machida Municipal Hospital, Machida, Tokyo 194-0023, Japan

Iterative reconstruction (IR) improves image quality compared with filtered back projection (FBP). This study investigated the usefulness of model-based IR (forward-projected model-based iterative reconstruction solution [FIRST]) in comparison with FBP and hybrid IR (adaptive iterative dose reduction three-dimensional processing [AIDR 3D]) in low-dose paranasal CT. Twenty-four patients with paranasal sinusitis who underwent standard-dose CT (120 kV) and low-dose CT (100 kV) scanning before and after medical treatment were enrolled. Standard-dose CT scans were reconstructed with FBP (FBP_{120}), and low-dose CT scans with FBP (FBP_{100}), AIDR 3D, and FIRST. The signal-to-noise ratio (SNR) and contrast-to-noise ratio (CNR) in three anatomical structures and effective doses were compared using Mann–Whitney *U* test. Two radiologists independently evaluated the visibility of 16 anatomical structures, overall image quality, and artifacts. Effective doses in low-dose CT were significantly reduced compared with those in standard-dose CT (0.24 vs 0.43 mSv, $p < 0.001$). FIRST achieved significantly higher SNR ($p < 0.01$, respectively) and CNR ($p < 0.001$, respectively) of evaluated structures and significant improvement in overall image quality ($p < 0.001$), artifacts ($p < 0.001$), and visibility related to muscles ($p < 0.05$) compared to FBP_{120}, FBP_{100}, and AIDR 3D. FIRST allowed radiation-dose reduction, while maintaining objective and subjective image quality in low-dose paranasal CT.

Key words: paranasal sinuses, iterative reconstruction, dose reduction, low dose

Paranasal computed tomography (CT) has been used to assess paranasal diseases, and in preoperative surgery planning and image-guided navigation. The high-resolution CT scans that have been developed to improve spatial resolution with thin slices require high radiation doses and thus increase the risk of radiation exposure. According to the principle of "as low as reasonably achievable" (ALARA), there is a need for CT scans with an ALARA optimal radiation dose that do not impair image quality.

Several methods are used to reduce the CT radiation dose: (1) decrease in tube current; (2) decrease in tube voltage; (3) use of noise reduction filters; and (4) high beam pitch [1-7]. However, radiation dose reduction results in image noise, which limits the filtered back projection (FBP) for CT scans. With the development of the CT reconstruction algorithm, two types of iterative reconstruction (IR), hybrid IR and model-based IR, have been applied to clinical practice as alternative

Received October 23, 2021; accepted April 6, 2022.
*Corresponding author. Phone: +81-44-977-8111; Fax: +81-44-977-2931
E-mail: m04149@yahoo.co.jp (H. Tomita)

Conflict of Interest Disclosures: No potential conflict of interest relevant to this article was reported.

methods of FBP [8-14]. One type of hybrid IR is adaptive iterative dose reduction three-dimensional processing (AIDR 3D; Canon Medical Systems), which can achieve lower image noise than FBP [5,6]. Additionally, a newer technique, a type of model-based IR, forward-projected model-based iterative reconstruction solution (FIRST; Canon Medical Systems), has been implemented to reduce image noise and maintain spatial resolution [9,10,12,14]. FIRST reduces image noise and streak artifacts compared with AIDR 3D [9,12,14]. To the best of our knowledge, however, no previous study has assessed the image quality of FBP, AIDR 3D, and FIRST in paranasal CT with different radiation doses.

In the present study, therefore, we evaluated the subjective and objective image quality in low-dose paranasal CT with FIRST, in comparison with standard-dose and low-dose CT with FBP and AIDR 3D, in clinical cases of paranasal sinusitis.

Materials and Methods

This retrospective study was approved by the institutional review board and the requirement for informed consent was waived.

Study patients. The inclusion criteria were as follows: (i) patients who underwent 320-row unenhanced CT for the assessment of paranasal sinusitis before and after medical treatment between August 2017 and June 2018; (ii) patients who underwent a second CT scan within 6 months after the start of medical treatment. Twenty-seven patients met these criteria. We excluded (i) patients who underwent previous surgery (n = 2) and (ii) a patient who experienced paranasal sinus trauma (n = 1). Thus, 24 patients were enrolled in this study.

CT protocol. All CT scans with volume scanning were performed using a 320-row CT scanner (Aquilion ONE; Canon Medical Systems) within the range of 12 cm above the inferior edge of the maxillary bone. The pre-treatment tube voltage of the initial CT scan was 120 kV, while that of the second scan was 100 kV. The other CT scanning parameters were the same for both scans: collimation, 240 × 0.5 mm; tube current, auto exposure control (AEC) with a kernel of FC 04 under the standard deviation (SD) of 9 HU for the standard-dose CT scans and 12 HU for the low-dose CT scans; gantry rotation time, 0.5 s. The imaging field of view (FOV) was 180 × 180 mm, and the pixel size was 0.35 × 0.35 mm.

Imaging reconstruction. All scan datasets were converted to axial and coronal CT scans with a slice thickness of 3 mm without any overlap. Image reconstruction was performed for the standard-dose CT scans with FBP (FBP_{120}), the low-dose CT scans with FBP (FBP_{100}), AIDR 3D (strong mode), and FIRST (BRAIN mode). All image assessments were performed on a commercially available workstation (Ziostation2; Ziosoft). A soft tissue condition for CT scans with FBP and AIDR 3D was reconstructed using a soft tissue kernel (FC04). Soft tissue conditions were displayed with 30/250 Hounsfield units (HU) of window level/width. A bony condition was set with edge enhancement and 600/3000 HU of window level/width.

Radiation dose. The radiation dose was expressed as the CT dose index volume ($CTDI_{vol}$) and dose-length product (DLP) taken from the patient's protocol. The effective radiation dose was calculated by multiplying DLP with a conversion factor of head range ($0.0019\ mSv \times mGy^{-1} \times cm^{-1}$).

Objective analysis. A circular region of interest (ROI; size, 5-10 mm^2) was placed on the targeted anatomical structures by a board-certified radiologist with 9 years of experience in head and neck radiology who was blinded to the identity of the patient. Image noise was defined as the standard deviation (SD) of attenuation values (HU) in the ventricle, pons, subcutaneous fat on the maxilla, and lateral pterygoid muscle. The signal-to-noise ratios (SNRs) for the pons, subcutaneous fat on the maxilla, and lateral pterygoid muscle were calculated as follows: SNR = mean HU/image noise. Contrast-to-noise ratios (CNRs) were calculated as follows: CNR = (HU [pons, subcutaneous fat on the maxilla, and lateral pterygoid muscle] – HU [ventricle])/SD [ventricle].

Subjective analysis. Two board-certified radiologists with 9 and 14 years of experience in head and neck radiology, respectively, who were blinded to the identity o the patients evaluated the visibility of the pons, eye globe, optic nerve, inferior orbital muscles, lateral pterygoid muscle, medial pterygoid muscle, masseter muscle, prevertebral muscle, levator veli palatini muscle, cribriform plate, lamina papyracea, middle turbinate, nasal septum, frontal sinus, spheno-ethmoid sinus, and maxillary sinus. Grading of visibility was performed using a 5-point scale (1 = undetectable;

2 = poor, major loss of visibility; 3 = fair, partial loss of visibility; 4 = good, minimal loss of visibility, but preservation of all anatomical details; 5 = excellent, visibility of all anatomical details). Additionally, the radiologists evaluated the overall image quality with a 5-point scale (1 = undiagnostic image quality; 2 = poor image quality; 3 = acceptable image quality; 4 = good image quality; 5 = excellent image quality) and artifacts with a 4-point scale (1 = severe artifact affecting diagnosis; 2 = moderate artifact affecting the structure visibility; 3 = slight artifact not affecting the visibility of any structure; 4=no detectable artifact).

Statistical analysis. Quantitative and qualitative image analyses of FBP_{120}, FBP_{100}, AIDR 3D, and FIRST were performed using the Mann–Whitney *U* test. The interobserver agreement was calculated using the interclass correlation coefficient (ICC), and values < 0.20 were interpreted as slight, 0.21-0.40 as fair, 0.41-0.60 as moderate, 0.61-0.80 as substantial, and > 0.81 as almost perfect. Statistical analysis was performed using JMP Pro 14.2.0 software (SAS Institute). A p value of < 0.05 was considered significantly different.

Results

Radiation dose. Table 1 shows the comparisons of the $CTDI_{vol}$, DLP, and effective dose between the standard-dose and low-dose CT. Significant differences in the $CTDI_{vol}$, DLP, and effective dose were observed between the standard-dose CT and low-dose CT ($p < 0.001$, for all).

Objective analysis. The image noise, SNR, and CNR of the targeted structures are summarized in Table 2. For each structure, FIRST showed a significantly higher SNR ($p < 0.01$, respectively) and CNR ($p < 0.001$, respectively) than FBP_{120}, FBP_{100}, or AIDR 3D. The SNR and CNR of the pons, subcutaneous muscle on the maxilla, and lateral pterygoid muscle of AIDR 3D were higher ($p < 0.001$, respectively) than those of FBP_{120} and FBP_{100}.

Subjective analysis. Table 3 compares the performance of the reconstruction algorithms during the subjective evaluations. FIRST showed significantly higher overall image quality than FBP_{120}, FBP_{100}, or AIDR 3D ($p < 0.001$, respectively). Additionally, FIRST achieved a significantly greater reduction in artifacts compared to FBP_{120}, FBP_{100}, and AIDR 3D ($p < 0.001$, respectively). All three reconstruction algorithms achieved sufficient visibility of all anatomical structures in the CT scans. Qualitative analyses of the targeted muscles showed the image quality was significantly higher with FIRST than with FBP_{120}, FBP_{100}, or AIDR 3D ($p < 0.05$, respectively). The ICCs for the qualitative analyses were 0.51-1.00. Figure 1 shows a representative case of lower image quality in the quantitative and qualitative analyses in CT with FBP_{120}, FBP_{100}, and AIDR 3D than FIRST.

Discussion

Low-dose paranasal CT was associated with a 44.2% reduction in radiation dose compared to the standard-dose CT in this study. FIRST achieved a significantly higher objective and subjective image quality than FBP_{120}, FBP_{100}, and AIDR 3D. Therefore, FIRST can provide a useful image quality in low-dose paranasal CT.

Cumulative radiation exposure can cause radiation-induced diseases through repetitive CTs [15, 16]. There is a tradeoff relationship between radiation dose and image noise in CT. Thus, different CT techniques for reducing the radiation dose while maintaining image quality have been evaluated. One of these techniques is IR, which has been classified into hybrid and model-based IR. Hybrid IR incorporates a noise reduction technique in the raw data and image data domain [17]. We expect that model-based IR will continue to improve image quality defects resulting from the lack of

Table 1 Comparisons of $CTDI_{vol}$, DLP, and the effective dose between the standard-dose and low-dose CT

	120 kVp	100 kVp	Reduction ratio	
CTDI (mGy)	17.10 ± 2.77	9.92 ± 1.59	41.83%	< 0.001
DLP (mGy × cm)	224.90 ± 48.12	128.30 ± 28.30	42.72%	< 0.001
Effective dose (mSv)	0.43 ± 0.09	0.24 ± 0.05	44.19%	< 0.001

$CTDI_{vol}$, the CT dose index volume; DLP, dose-length product.
*indicates a significant difference.

Table 2 Comparisons of objective image quality between FBP_{120}, FBP_{100}, AIDR 3D, and FIRST

		FBP_{120}	FBP_{100}	AIDR 3D	FIRST	FBP_{120} vs FBP_{100}	AIDR 3D vs FBP_{120}	AIDR 3D vs FBP_{100}	FBP_{120} vs FIRST	FBP_{100} vs FIRST	AIDR 3D vs FIRST
Attenuation values	Ventricle	0.85 ± 3.48	−1.46 ± 3.43	−1.85 ± 4.03	0.85 ± 3.48	0.027*	0.11	0.67	<0.001*	0.037*	0.015*
	Pons	27.34 ± 3.20	29.69 ± 5.08	29.40 ± 4.63	34.28 ± 5.51	0.068*	0.08	0.74	<0.001*	0.004*	0.002*
	Subcutaneous fat on the maxilla	−117.30 ± 11.17	−124.75 ± 11.15	−125.16 ± 11.22	−114.41 ± 10.78	0.003*	0.003*	0.80	0.32	0.001*	0.001*
	Lateral pterygoid muscle	50.99 ± 6.32	55.93 ± 6.39	56.79 ± 5.62	60.80 ± 6.51	0.009*	0.003*	0.54	<0.001*	0.003*	0.01*
Noise	Ventricle	9.66 ± 1.66	12.31 ± 2.03	7.06 ± 1.56	4.78 ± 1.42	<0.001*	<0.001*	<0.001*	<0.001*	<0.001*	<0.001*
	Pons	9.75 ± 1.43	13.27 ± 1.70	7.23 ± 1.26	6.22 ± 1.47	<0.001*	<0.001*	<0.001*	<0.001*	<0.001*	0.014*
	Subcutaneous fat on the maxilla	8.05 ± 2.42	9.51 ± 1.85	6.90 ± 1.75	5.57 ± 1.67	<0.001*	0.004*	<0.001*	<0.001*	<0.001*	0.001*
	Lateral pterygoid muscle	9.16 ± 1.38	11.11 ± 1.97	6.81 ± 1.41	5.80 ± 1.40	<0.001*	<0.001*	<0.001*	<0.001*	<0.001*	<0.001*
SNR	Ventricle	−0.12 ± 0.33	−0.40 ± 0.33	−0.29 ± 0.62	0.13 ± 0.57	0.008*	0.33	0.39	0.002*	<0.001*	<0.001*
	Pons	2.78 ± 0.60	2.23 ± 0.49	4.12 ± 1.16	6.00 ± 2.13	<0.001*	<0.001*	<0.001*	<0.001*	<0.001*	<0.001*
	Subcutaneous fat on the maxilla	15.69 ± 4.32	13.68 ± 3.29	19.56 ± 6.32	22.90 ± 9.08	<0.001*	<0.001*	<0.001*	<0.001*	<0.001*	0.006*
	Lateral pterygoid muscle	5.88 ± 1.58	4.78 ± 1.04	8.76 ± 2.47	13.89 ± 5.81	0.08	<0.001*	<0.001*	<0.001*	<0.001*	<0.001*
CNR	Pons	3.35 ± 0.97	2.59 ± 0.63	4.64 ± 1.31	7.57 ± 2.56	0.004*	<0.001*	<0.001*	<0.001*	<0.001*	<0.001*
	Subcutaneous fat on the maxilla	12.24 ± 3.28	10.28 ± 1.85	18.20 ± 3.82	26.41 ± 8.88	<0.001*	<0.001*	<0.001*	<0.001*	<0.001*	<0.001*
	Lateral pterygoid muscle	5.88 ± 1.58	4.78 ± 1.04	8.76 ± 2.47	13.89 ± 5.81	<0.001*	<0.001*	<0.001*	<0.001*	<0.001*	<0.001*

FBP_{120}, FBP with 120 kV; FBP_{100}, FBP with 100 kV; AIDR 3D, adaptive iterative dose reduction three dimensional processing; FIRST, forward-projected model-based iterative reconstruction solution; SD, standard deviation; SNR, signal-to-noise ratio; CNR, contrast-to-noise ratio.
*indicates a significant difference.

Table 3 Comparisons of subjective image quality between FBP_{120}, FBP_{100}, AIDR 3D, and FIRST

	FBP_{120}	FBP_{100}	AIDR 3D	FIRST	FBP_{120} vs FBP_{100}	AIDR 3D vs FBP_{120}	AIDR 3D vs FBP_{100}	FBP_{120} vs FIRST	FBP_{100} vs FIRST	AIDR 3D vs FIRST
Pons	3.63 ± 0.57	3.17 ± 0.47	3.63 ± 0.53	3.71 ± 0.50	<0.001*	0.80	<0.001*	0.29	<0.001*	0.40
Eye globe	4.04 ± 0.20	3.88 ± 0.44	4.13 ± 0.33	4.19 ± 0.46	0.019*	0.14	0.003*	0.037*	0.001*	0.41
Optic nerve	4.00 ± 0.41	3.75 ± 0.53	4.04 ± 0.50	4.23 ± 0.66	0.011*	0.65	0.007*	0.032*	<0.001*	0.10
Inferior rectus muscle	4.27 ± 0.57	4.13 ± 0.61	4.45 ± 0.50	4.71 ± 0.54	0.24	0.12	0.008*	<0.001*	<0.001*	0.009*
Lateral pterygoid muscle	4.08 ± 0.40	4.06 ± 0.24	4.54 ± 0.50	4.79 ± 0.41	0.73	<0.001*	<0.001*	<0.001*	<0.001*	0.01*
Medial pterygoid muscle	3.83 ± 0.43	3.94 ± 0.24	4.23 ± 0.56	4.81 ± 0.39	0.18	<0.001*	0.001*	<0.001*	<0.001*	<0.001*
Masseter muscle	4.04 ± 0.20	3.96 ± 0.20	4.27 ± 0.45	4.94 ± 0.24	0.048*	0.002*	<0.001*	<0.001*	<0.001*	<0.001*
Prevertebral muscle	4.23 ± 0.52	4.08 ± 0.35	4.65 ± 0.48	4.92 ± 0.35	0.09	<0.001*	<0.001*	<0.001*	<0.001*	<0.001*
Levator veli palatini muscle	3.94 ± 0.32	3.97 ± 0.39	4.60 ± 0.49	4.90 ± 0.37	0.59	<0.001*	<0.001*	<0.001*	<0.001*	<0.001*
All bony structures	5.00 ± 0.00	5.00 ± 0.00	5.00 ± 0.00	5.00 ± 0.00	1.00	1.00	1.00	1.00	1.00	1.00
Overall image quality	3.85 ± 0.36	3.38 ± 0.49	4.19 ± 0.39	4.58 ± 0.65	<0.001*	<0.001*	<0.001*	<0.001*	<0.001*	<0.001*
Artifact	3.00 ± 0.00	3.00 ± 0.00	3.25 ± 0.44	3.83 ± 0.52	1.00	<0.001*	0.012*	<0.001*	<0.001*	<0.001*

FBP_{120}, FBP with 120 kV; FBP_{100}, FBP with 100 kV; AIDR 3D, adaptive iterative dose reduction three dimensional processing; FIRST, forward-projected model-based iterative reconstruction solution.
*indicates a significant difference.

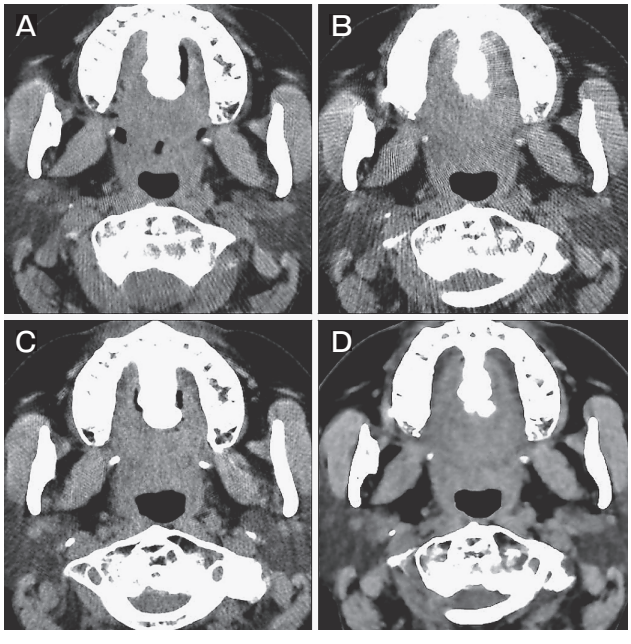

Fig. 1 A 62-year-old female patient with paranasal sinusitis. CT images are reconstructed with (**A**) filter-back projection in standard-dose CT (FBP_{120}); (**B**) filter-back projection (FBP_{100}); (**C**) adaptive iterative dose reduction three-dimensional processing (AIDR 3D); (**D**) forward-projected model-based iterative reconstruction solution (FIRST) in low-dose CT. The artifacts and image noise were reduced in CT with FIRST compared with FBP_{120}, FBP_{100}, and AIDR 3D at the level of the maxillary bone.

sufficient photons. Model-based IR has been shown not to impair image quality in low-dose CT scans of the neck, chest, and abdomen [9,13,18-20]. The performance of low-radiation-dose paranasal CT was reported in previous studies. May *et al.* described that a noise reduction filter reduced the radiation dose and improved image noise in low-dose paranasal CT [3]. However, most CT scanners do not have noise reduction filters [3]. Some studies have described that CT scans with a low tube voltage of 70 kV without IR showed acceptable subjective image quality equivalent to that of CT scans with 120 kV as a standard radiation dose [7,21]. However, they also found that image noise was significantly higher in CT scans with 70 kV than 120 kV, since the reducing radiation dose increased the image noise. IR has also been applied to low-dose paranasal CT. Schaafs *et al.* and Schulz *et al.* have described that hybrid IR reduced radiation doses while maintaining image quality compared to FBP in paranasal CT scans using different tube currents and tube voltages [10,11]. Hoxworth *et al.* reported that VEO (GE Healthcare), one of the model-based IRs, significantly reduced image noise compared to FBP in paranasal CT with 20 mA and 120 kV (2.9 mGy) [22]. However, to our knowledge there has been no comparison between hybrid IR and model-based IR in the context of paranasal CT. Additionally, the detailed information of model-based IR algorithms provided by CT

vendors remains largely hidden. Thus, each model-based IR in paranasal CT must be evaluated independently, with optimal CT parameters and radiation doses. In our study, FIRST was associated with higher image quality than FBP_{120}, FBP_{100}, and AIDR 3D. Regarding objective and subjective analyses in low-dose CT scans, FIRST was superior to FBP_{100} and AIDR 3D due to its reduction of image noise and artifacts. FIRST incorporates an algorithm that eliminates the beam-hardening artifact, avoids raw data undershoot, and shows fewer artifacts than AIDR 3D. FIRST had a reconstruction time of approximately 190 seconds in this study. However, we believe that the time constraints will be less important in a clinic.

Our study has some limitations. First, we did not determine the optimal tube voltage for low-dose paranasal CT. Second, the small cohort size in this study limited our statistical power. Third, the ROI was manually placed to evaluate objective image quality. Fourth, different SD settings were used for AEC. Although the consistent use of a single CT protocol would be preferable, the use of FIRST in low-dose CT would further improve the image quality under the same SD settings, because the SD was higher on low-dose CT than that on standard-dose CT. Fifth, soft tissue and bony conditions were displayed with fixed window levels/widths. The images with different tube voltages might show different visibility. Additional and well-powered studies with optimized settings will be needed.

In conclusion, FIRST was associated with improved image quality in low-dose CT. FIRST demonstrated higher image noise reduction than either FBP or AIDR 3D.

References

1. Marmolya G, Wiesen EJ, Yagan R, Haria CD and Shah AC: Paranasal sinuses: low-dose CT. Radiology (1991) 181: 689–691.
2. Lell MM, Wildberger JE, Alkadhi H, Damilakis J and Kachelriess M: Evolution in Computed Tomography: The Battle for Speed and Dose. Invest Radiol (2015) 50: 629–644.
3. May MS, Brand M, Lell MM, Sedlmair M, Allmendinger T, Uder M and Wuest W: Radiation dose reduction in parasinus CT by spectral shaping. Neuroradiology (2017) 59: 169–176.
4. Wuest W, May M, Saake M, Brand M, Uder M and Lell M: Low-Dose CT of the Paranasal Sinuses: Minimizing X-Ray Exposure with Spectral Shaping. Eur Radiol (2016) 26: 4155–4161.
5. Nagatani Y, Takahashi M, Murata K, Ikeda M, Yamashiro T, Miyara T, Koyama H, Koyama M, Sato Y, Moriya H, Noma S, Tomiyama N, Ohno Y and Murayama S: Lung nodule detection performance in five observers on computed tomography (CT) with adaptive iterative dose reduction using three-dimensional processing (AIDR 3D) in a Japanese multicenter study: Comparison between ultra-low-dose CT and low-dose CT by receiver-operating characteristic analysis. Eur J Radiol (2015) 84: 1401–1412.
6. Yamashiro T, Miyara T, Honda O, Kamiya H, Murata K, Ohno Y, Tomiyama N, Moriya H, Koyama M, Noma S, Kamiya A, Tanaka Y and Murayama S: Adaptive Iterative Dose Reduction Using Three Dimensional Processing (AIDR3D) improves chest CT image quality and reduces radiation exposure. PLoS ONE (2014) 9: e105735.
7. Bodelle B, Wichmann JL, Klotz N, Lehnert T, Vogl TJ, Luboldt W and Schulz B: Seventy kilovolt ultra-low dose CT of the paranasal sinus: first clinical results. Clin Radiol (2015) 70: 711–715.
8. Örgel A, Bier G, Hennersdorf F, Richter H, Ernemann U and Hauser TK: Image Quality of CT Angiography of Supra-Aortic Arteries: Comparison Between Advanced Modelled Iterative Reconstruction (ADMIRE), Sinogram Affirmed Iterative Reconstruction (SAFIRE) and Filtered Back Projection (FBP) in One Patients' Group. Clin Neuroradiol (2020) 30: 101–107.
9. Hassani C, Ronco A, Prosper AE, Dissanayake S, Cen SY and Lee C: Forward-Projected Model-Based Iterative Reconstruction in Screening Low-Dose Chest CT: Comparison With Adaptive Iterative Dose Reduction 3D. AJR Am J Roentgenol (2018) 211: 548–556.
10. Schaafs LA, Lenk J, Hamm B and Niehues SM: Reducing the dose of CT of the paranasal sinuses: potential of an iterative reconstruction algorithm. Dentomaxillofac Radiol (2016) 45: 20160127.
11. Schulz B, Beeres M, Bodelle B, Bauer R, Al-Butmeh F, Thalhammer A, Vogl TJ and Kerl JM: Performance of iterative image reconstruction in CT of the paranasal sinuses: a phantom study. AJNR Am J Neuroradiol (2013) 34: 1072–1076.
12. Wu R, Hori M, Onishi H, Nakamoto A, Fukui H, Ota T, Nishida T, Enchi Y, Satoh K and Tomiyama N: Effects of reconstruction technique on the quality of abdominal CT angiography: A comparison between forward projected model-based iterative reconstruction solution (FIRST) and conventional reconstruction methods. Eur J Radiol (2018) 106: 100–105.
13. Yamada Y, Jinzaki M, Niijima Y, Hashimoto M, Yamada M, Abe T and Kuribayashi S: CT Dose Reduction for Visceral Adipose Tissue Measurement: Effects of Model-Based and Adaptive Statistical Iterative Reconstructions and Filtered Back Projection. AJR Am J Roentgenol (2015) 204: W677–683.
14. Yokomachi K, Tatsugami F, Higaki T, Kume S, Sakamoto S, Okazaki T, Kurisu K, Nakamura Y, Baba Y, Iida M and Awai K: Neointimal formation after carotid artery stenting: phantom and clinical evaluation of model-based iterative reconstruction (MBIR). Eur Radiol (2019) 29: 161–167.
15. Berrington de González A, Mahesh M, Kim KP, Bhargavan M, Lewis R, Mettler F and Land C: Projected cancer risks from computed tomographic scans performed in the United States in 2007. Arch Intern Med (2009) 169: 2071–2077.
16. Brenner DJ and Hall EJ: Computed tomography--an increasing source of radiation exposure. N Engl J Med (2007) 357: 2277–2284.
17. Willemink MJ and Noël PB: The evolution of image reconstruction for CT-from filtered back projection to artificial intelligence. Eur Radiol (2019) 29: 2185–2195.
18. Nakamoto A, Kim T, Hori M, Onishi H, Tsuboyama T, Sakane M, Tatsumi M and Tomiyama N: Clinical evaluation of image quality and radiation dose reduction in upper abdominal computed tomog-

raphy using model-based iterative reconstruction; comparison with filtered back projection and adaptive statistical iterative reconstruction. Eur J Radiol (2015) 84: 1715–1723.
19. Scholtz JE, Kaup M, Hüsers K, Albrecht MH, Bodelle B, Metzger SC, Kerl JM, Bauer RW, Lehnert T, Vogl TJ and Wichmann JL: Advanced Modeled Iterative Reconstruction in Low-Tube-Voltage Contrast-Enhanced Neck CT: Evaluation of Objective and Subjective Image Quality. AJNR Am J Neuroradiol (2016) 37: 143–150.
20. Schmid AI, Uder M and Lell MM: Reaching for better image quality and lower radiation dose in head and neck CT: advanced modeled and sinogram-affirmed iterative reconstruction in combination with tube voltage adaptation. Dentomaxillofac Radiol (2017) 46: 20160131.
21. Gnannt R, Winklehner A, Goetti R, Schmidt B, Kollias S and Alkadhi H: Low kilovoltage CT of the neck with 70kVp: comparison with a standard protocol. AJNR Am J Neuroradiol (2012) 33: 1014–1019.
22. Hoxworth JM, Lal D, Fletcher GP, Patel AC, He M, Paden RG and Hara AK: Radiation dose reduction in paranasal sinus CT using model-based iterative reconstruction. AJNR Am J Neuroradiol (2014) 35: 644–649.